Effects of structural uncertainties on the nonlinear elastic post-buckling behavior of a cylindrical shell. Stochastic computational modeling and comparison with experiments

Evangéline Capiez-Lernout, Christian Soize, M. P. Mignolet

Proceedings of the 8th International Conference on Structural Dynamics, EURODYN 2011
Leuven, Belgium, 4-6 July 2011
G. De Roeck, G. Degrande, G. Lombaert, G. Müller (eds.)
ISBN 978-90-760-1931-4

Effect of structural uncertainties on the nonlinear elastic behavior of a curved beam. Stochastic computational modeling and comparison with simulated experiments.

Capiez-Lernout, E.[1], Soize, C. [1], Mignolet, M.P. [2]
[1] Université Paris-Est, Laboratoire Modélisation et Simulation Multi-Echelle, MSME UMR 8208 CNRS, 5 bd Descartes, 77454 Marne-la-Vallée, France
[2] Arizona State University,Tempe, Faculties of Mechanical and Aerospace Engineering, Arizona 85287-6106, USA
email: evangeline.capiezlernout@univ-paris-est.fr,christian.soize@univ-paris-est.fr,marc.mignolet@asu.edu

ABSTRACT: A methodology for analyzing the response of geometrically nonlinear structural systems in presence of both system parameters uncertainties and model uncertainties is presented in the context of the robust identification of uncertain nonlinear computational models using experiments. This methodology requires the knowledge of a reference calculation issued from the mean model in order to obtain the POD-basis used for the construction of the mean reduced nonlinear computational model. This explicit construction is carried out in the context of three-dimensional solid finite elements. This allows the uncertain nonlinear computational model to be constructed in any general case with the nonparametric probabilistic approach. A numerical example is then carried out in order to show the efficiency of the method.

KEY WORDS: uncertainties, geometrical nonlinearities, POD, robust updating, post-buckling

1 INTRODUCTION

In structural mechanics, a recent challenge of interest is to have advanced numerical methodologies for constructing robust computational models in order to efficiently predict the mechanical behavior of structures. In numerous industrial applications, the effects of geometrical nonlinearities induced by large strains and by large displacements have to be taken into account in the numerical modeling. For instance, such nonlinear mechanical behavior is exhibited in aeronautics for the case of helicopter rotating blades [1], [2] or in automotive or aerospatial industries for the case of slender beams or thin shells [3], [4], [5]. In the context of complex structures, large finite element computational models are needed. Given the numerical difficulties inherent to the complexity of such computational models, many recent researches have focused on the construction of reduced order models in this nonlinear context [6], [7]. In particular, the ELSTEP procedure [8], [9] has been developed in order to explicitly construct all the linear, quadratic, cubic stiffness terms related to reduced nonlinear models. The methodology is based on the smart use of an industrial finite element code for which no further numerical developments are needed. It only requires a series of basic nonlinear numerical calculations with judicious prescribed displacements taken as a linear combination of given basis vectors.

Moreover, deterministic nonlinear computational models are in general not sufficient to accurately predict the mechanical behavior of such complex structures. The uncertainties have then to be taken into account in the computational models by using probabilistic models as soon as the probability theory can be used. Let us recall that there exist two classes of uncertainties: (1) the system parameter uncertainties result from the variability of the parameters of the computational model induced for instance by the manufacturing process, (2) the model uncertainties are the features of the mechanical system not captured by the computational model, e.g. the introduction of reduced kinematics in the numerical modeling. Parametric probabilistic approaches are particularly adapted to take into account system parameter uncertainties as shown in [10], [11] is the context of the post-buckling of cylindrical shells. This last decade, the nonparametric probabilistic approach adapted to the modeling of both model uncertainties and system parameter uncertainties has been introduced in [12], [13] for the linear case and has been extended more recently in [9], [14] in the context of geometrical nonlinearities. In the present paper, a direct procedure is proposed in the context of geometrical nonlinear structural mechanical systems. In this methodology, the explicit construction of the uncertain nonlinear computational model is proposed for any type of structure modeled with three-dimensional solid finite elements.

In the first Section, the equations of the geometrical nonlinear problem are written in the context of a total Lagrangian formulation. The second Section is devoted to the construction of a mean reduced nonlinear computational model required by the implementation of the nonparametric probabilistic approach. This mean reduced nonlinear computational model is obtained using the Proper Orthogonal Decomposition method known to be particularly efficient in nonlinear cases [6]. The POD-basis is then easily deduced from a reference solution taken as the deterministic response of the structure. The mean reduced nonlinear computational model, which results from the projection of all the linear, quadratic and cubic stiffness terms on this POD-basis is then explicitly constructed in the context of three-dimensional solid finite elements. The third Section is devoted to the construction of the uncertain nonlinear computational model using the nonparametric probabilistic approach. Such nonparametric probabilistic approach is based on the construction of a probability model for random matrices with values in the set of symmetric positive-definite matrices whose mean value is deduced from the mean reduced computational model. Let us recall that the nonlinear quadratic stiffness term of the mean reduced nonlinear computational model is defined as the sum of three nonlinear terms. In the present geometrical nonlinear context, the nonparametric probabilistic model is implemented from a deterministic symmetric positive-definite matrix whose components are notably described by each of these three nonlinear terms. Note that its explicit construction is then needed. In the fourth Section, the procedure for the robust identification of the uncertain nonlinear computational model with respect to available experimental responses is carried out [15], [16]. Finally, the fifth Section is devoted to a numerical example in order to demonstrate the efficiency of the proposed methodology.

2 FORMULATION OF THE GEOMETRIC NONLINEAR PROBLEM

The structure under consideration is made up of a linear elastic material and is assumed to undergo large deformations induced by geometrical nonlinearity. Let Ω be the three-dimensional bounded domain of the physical space $\mathbb{R}^3$ corresponding to the reference configuration taken as a natural state without prestresses. The boundary $\partial\Omega$ is such that $\partial\Omega = \Gamma \bigcup \Sigma$ with $\Gamma \bigcap \Sigma = \emptyset$ and the external unit normal to boundary $\partial\Omega$ is denoted as $\mathbf{n}$. The boundary part Γ corresponds to the fixed part of the structure whereas the boundary part Σ is submitted to an external surface force field. A total Lagrangian formulation is chosen. Consequently, the mechanical equations are written with respect to the reference configuration. Let $\mathbf{x}$ be the position of a point belonging to domain Ω. The displacement field expressed with respect to the reference configuration is denoted as $\mathbf{u}(\mathbf{x})$. It should be noted that the surface force field $\mathbf{G}(\mathbf{x})$ acting on boundary Σ and that the body force field $\mathbf{g}(\mathbf{x})$ acting on domain Ω corresponds to the Lagrangian transport of the physical surface force field and to the physical body force field applied on the deformed configuration into the reference configuration. Let $\mathcal{C}$ be the admissible space defined by

$$\mathcal{C} = \{\mathbf{v} \in \Omega, \mathbf{v} \text{ sufficiently regular }, \mathbf{v} = \mathbf{0} \textbf{ on } \Gamma\} \quad . \tag{1}$$

The weak formulation of the geometric nonlinear static boundary problem consists in finding the unknown displacement field $\mathbf{u}$ of admissible space $\mathcal{C}$ such that, for any admissible displacement field $\mathbf{v} \in \mathcal{C}$

$$\int_\Omega v_{i,k} F_{ij} S_{jk} \, d\mathbf{x} = \int_\Omega v_i g_i \, d\mathbf{x} + \int_\Sigma v_i G_i \, d\mathbf{s} \quad , \tag{2}$$

in which $\mathbb{F}$ is the deformation gradient tensor whose components F_{ij} are defined by

$$F_{ij} = u_{i,j} + \delta_{ij} \quad , \tag{3}$$

in which δ_{ij} is the Kronecker symbol such that $\delta_{ij} = 1$ if $i = j$ and $\delta_{ij} = 0$ if not, and where $\mathbb{S}$ is the second Piola-Kirchoff symmetric stress tensor defined for any elastic material by the linear relation

$$S_{ij} = a_{ijkl} E_{kl} \quad . \tag{4}$$

In Eq. (4), the fourth order elasticity tensor $\mathbb{a}$ satisfies the classical symmetry and positive definiteness properties. The Green strain tensor $\mathbb{E}$ is then written as the sum of a linear term and of a nonlinear term such that

$$E_{ij} = \varepsilon_{ij} + \eta_{ij} \quad , \tag{5}$$

in which

$$\varepsilon_{ij} = \frac{1}{2}\left(u_{i,j} + u_{j,i}\right) \quad \text{and} \quad \eta_{ij} = \frac{1}{2} u_{s,i} u_{s,j} \quad . \tag{6}$$

The weak formulation Eq. (2) is reformulated as finding the unknown displacement field $\mathbf{u}$ of admissible space $\mathcal{C}$ such that, for any admissible displacement field $\mathbf{v} \in \mathcal{C}$ we have

$$k^{(1)}(\mathbf{u},\mathbf{v}) + k^{(2)}(\mathbf{u},\mathbf{u},\mathbf{v}) + k^{(3)}(\mathbf{u},\mathbf{u},\mathbf{u},\mathbf{v}) = l(\mathbf{v}) \quad , \tag{7}$$

in which the multilinear forms $l(\mathbf{v})$, $k^{(1)}(\mathbf{u},\mathbf{v})$, $k^{(2)}(\mathbf{u},\mathbf{u},\mathbf{v})$ and $k^{(3)}(\mathbf{u},\mathbf{u},\mathbf{u},\mathbf{v})$ are defined for all $\mathbf{u},\mathbf{v} \in \mathcal{C}$ by

$$l(\mathbf{v}) = \int_\Omega v_i g_i \, d\mathbf{x} + \int_\Sigma v_i G_i \, d\mathbf{s} \quad , \tag{8}$$

$$k^{(1)}(\mathbf{u},\mathbf{v}) = \int_\Omega a_{jklm} \varepsilon_{lm}(\mathbf{u}) \, \varepsilon_{jk}(\mathbf{v}) \, d\mathbf{x} \quad , \tag{9}$$

$$k^{(2)}(\mathbf{u},\mathbf{u},\mathbf{v}) = \int_\Omega a_{jklm} \eta_{lm}(\mathbf{u}) \varepsilon_{jk}(\mathbf{v}) d\mathbf{x} + \int_\Omega a_{jklm} u_{s,j} v_{s,k} \varepsilon_{lm}(\mathbf{u}) d\mathbf{x} \tag{10}$$

$$k^{(3)}(\mathbf{u},\mathbf{u},\mathbf{u},\mathbf{v}) = \int_\Omega a_{jklm} \, u_{s,j} \, v_{s,k} \, \eta_{lm}(\mathbf{u}) \, d\mathbf{x} \quad . \tag{11}$$

3 CONSTRUCTION OF A MEAN REDUCED COMPUTATIONAL MODEL FOR THE GEOMETRICAL NONLINEAR PROBLEM

This Section concerns the construction of the mean reduced computational model adapted to the geometrical nonlinear context. The methodology is based on the explicit construction of each term constituting this mean reduced nonlinear computational model. It is recalled that such mean reduced nonlinear computational model is required by the nonparametric probabilistic modeling of uncertainties. First, the general equations yielding the mean reduced nonlinear computational model are written for any given projection basis. Then, the Proper Orthogonal Decomposition method is used for constructing the projection basis in the context of large finite elements systems [17], [6]. This POD-basis is deduced from a reference calculation using a finite element code. Finally, each linear, quadratic and cubic stiffness component constituting the mean reduced nonlinear computational model is explicitly constructed in the context of three-dimensional solid finite elements.

3.1 General equations of the mean reduced model

Let $\varphi^\alpha(\mathbf{x})$, $\alpha = \{1,\ldots,N\}$, be a given set of basis functions such that

$$\mathbf{u}(\mathbf{x}) = \sum_{\beta=1}^{N} \varphi^\beta(\mathbf{x}) \, q_\beta \quad , \tag{12}$$

in which the $\mathbb{R}^N$-vector $\mathbf{q} = (q_1,\dots,q_N)$ is the vector of the generalized coordinates. Let $\mathbf{v}(\mathbf{x})$ be a test function such that

$$\mathbf{v}(\mathbf{x}) = \varphi_\alpha(\mathbf{x})\, q_\alpha \tag{13}$$

Replacing Eq.(13) in Eq.(7) yields the following set of nonlinear equations

$$\mathcal{K}^{(1)}_{\alpha\beta}\, q_\beta + \mathcal{K}^{(2)}_{\alpha\beta\gamma} q_\beta\, q_\gamma + \mathcal{K}^{(3)}_{\alpha\beta\gamma\delta}\, q_\beta\, q_\gamma q_\delta = \mathcal{F}_\alpha \quad , \tag{14}$$

in which

$$\mathcal{K}^{(1)}_{\alpha\beta} = \int_\Omega a_{jklm}\, \varphi^\alpha_{j,k}\, \varphi^\beta_{l,m}\, d\mathbf{x} \quad , \tag{15}$$

$$\mathcal{K}^{(2)}_{\alpha\beta\gamma} = \frac{1}{2}\left(\hat{\mathcal{K}}^{(2)}_{\alpha\beta\gamma} + \hat{\mathcal{K}}^{(2)}_{\beta\gamma\alpha} + \hat{\mathcal{K}}^{(2)}_{\gamma\alpha\beta}\right) \quad , \tag{16}$$

$$\hat{\mathcal{K}}^{(2)}_{\alpha\beta\gamma} = \int_\Omega a_{jklm}\, \varphi^\alpha_{j,k}\, \varphi^\beta_{s,l}\, \varphi^\gamma_{s,m}\, d\mathbf{x} \quad , \tag{17}$$

$$\hat{\mathcal{K}}^{(3)}_{\alpha\beta\gamma\delta} = \int_\Omega a_{jklm}\, \varphi^\alpha_{r,j}\, \varphi^\beta_{r,k}\, \varphi^\gamma_{s,l}\, \varphi^\delta_{s,m}\, d\mathbf{x} \quad , \tag{18}$$

$$\mathcal{F}_\alpha = \int_\Sigma G_i \varphi^\alpha_i\, d\mathbf{s} + \int_\Omega g_i \varphi^\alpha_i\, d\mathbf{x} \quad . \tag{19}$$

It can easily be seen that the symmetry properties of the fourth order elasticity tensor yield the following properties

$$\mathcal{K}^{(1)}_{\alpha\beta} = \mathcal{K}^{(1)}_{\beta\alpha} \tag{20}$$

$$\hat{\mathcal{K}}^{(2)}_{\alpha\beta\gamma} = \hat{\mathcal{K}}^{(2)}_{\alpha\gamma\beta} \tag{21}$$

$$\mathcal{K}^{(2)}_{\alpha\beta\gamma} = \mathcal{K}^{(2)}_{\beta\gamma\alpha} = \mathcal{K}^{(2)}_{\gamma\alpha\beta} \tag{22}$$

$$\mathcal{K}^{(3)}_{\alpha\beta\gamma\delta} = \mathcal{K}^{(3)}_{\alpha\beta\delta\gamma} = \mathcal{K}^{(3)}_{\beta\alpha\gamma\delta} = \mathcal{K}^{(3)}_{\gamma\delta\alpha\beta} \tag{23}$$

Moreover, using the positive-definite property of the fourth-order elasticity tensor, it can be shown that the tensors $\mathcal{K}^{(1)}_{\alpha\beta}$ and $\mathcal{K}^{(3)}_{\alpha\beta\delta\gamma}$ are positive-definite.

3.2 Numerical construction of the reduced order basis using Proper Orthogonal Decomposition

The set of basis vectors used for constructing the mean reduced nonlinear computational model is obtained with the Proper Orthogonal Decomposition method which is known to be efficient for nonlinear cases. The determination of this basis necessarily requires a reference response. Indeed such basis is defined by the eigenvalue problem of the spatial correlation operator related to the displacement field of this reference response. It should be noted that this basis does not only depend on the operators of the computational model but also strongly depends on the external applied loads used for exciting the structure. Below, the numerical construction of the POD-basis is summarized in the context of the finite element method. The finite element discretization of Eq. (7) can be written as

$$[K^{(1)}]\mathbf{u} + \mathbf{f}^{NL}(\mathbf{u}) = \mathbf{f} \quad , \tag{24}$$

in which the $\mathbb{R}^n$-vector $\mathbf{u}$ is the vector of the unknown displacements. In Eq. (24), the $(n\times n)$ symmetric positive definite matrix $[K^{(1)}]$ is the linear finite element stiffness matrix, the $\mathbb{R}^n$-vector $\mathbf{f}^{NL}(\mathbf{u})$ is the vector of the restoring forces induced by the geometrical nonlinear effects and the $\mathbb{R}^n$-vector $\mathbf{f}$ is the vector of the external applied loads. It should be noted that there are specific numerical algorithms for solving this nonlinear equation (see for instance [18]) which are particularly efficient as the curvature of the nonlinear response changes (see for instance [19] for algorithms based on arc-length methods or [20] for algorithms based on asymptotic methods).

Let $s_j \in [0,1]$, $j \in \{1,\dots,p\}$ with $s_j < s_{j+1}$ be the scalar denoting the incremental weight number j of the external load vector $\mathbf{f}$. The $(n\times p)$ real matrix $[V]$ is then introduced as

$$[V]_{ij} = u_i(s_j)\sqrt{\Delta s_j} \quad , \quad \Delta s_j = s_j - s_{j-1} \text{ with } s_0 = 0 \quad . \tag{25}$$

The spatial correlation matrix related to the nonlinear reference response is defined by the symmetric positive-definite $(n\times n)$ real matrix $[A]$ such that

$$[A] = [V]\,[V]^T \quad . \tag{26}$$

The POD-basis is then obtained in solving the following eigenvalue problem

$$[A]\,[\Phi] = [\Phi]\,[\Lambda] \quad , \tag{27}$$

in which $[\Lambda]$ is the diagonal matrix whose components are the eigenvalues ordered by decreasing values and where $[\Phi]$ is the modal matrix whose columns are the POD-basis vectors. It should be noted that such numerical construction can not be carried out as the dimension n of the system increases. The following methodology introduced by [17], [6] and adapted to large computational models is then used. The singular value decomposition of matrix $[V]$ is written as

$$[V] = [B]\,[S]\,[C] \quad , \tag{28}$$

in which $[S] = [\Lambda]^{1/2}$ and where the columns of the $(n\times n)$ real matrices $[B]$ and $[C]$ are the left and right singular vectors related to the corresponding singular values. Let $[B]^N$ be the $(n\times N)$ matrix issued from the truncation of matrix $[B]$ with respect to the N largest singular values. Matrix $[B]^N$ can be easily computed. The $(N\times N)$ symmetric positive-definite real matrix $[\mathcal{A}]^N$ is then introduced as

$$[\mathcal{A}^N] = [W^N]\,[W^N]^T \quad , \quad \text{with } [W^N] = [B^N]^T\,[V] \quad . \tag{29}$$

Denoting as $[\Phi^N]$ the $(n\times N)$ real matrix defined by the truncation of matrix $[\Phi]$ with respect to the N largest singular values, we then have

$$[\Phi^N] = [B^N]\,[\Psi^N] \quad , \tag{30}$$

in which $[\Psi^N]$ is the modal matrix solution of the eigenvalue problem

$$[\mathcal{A}^N]\,[\Psi^N] = [\Psi^N]\,[\Lambda^N] \quad , \tag{31}$$

where $[\Lambda^N]$ is the $(N\times N)$ real diagonal matrix defined as the truncation of matrix $[\Lambda]$ with respect to the N largest singular values.

3.3 Construction of the mean reduced nonlinear computational model

In this subsection, the mean reduced nonlinear computational model is explicitly constructed from the knowledge of the POD-basis. The construction is carried out in the context of the three-dimensional finite element method. The finite elements used are isoparametric solid finite elements with 8 nodes and the numerical integration is carried out with r Gauss integration points.

Let $[D]$ be the (6×6) real matrix which represents the usual Hooke matrix related to the fourth-order elasticity tensor. For the considered isoparametric finite element, the displacement field $\tilde{\mathbf{u}}(\mathbf{y})$ with $\mathbf{y}\in[-1,1]^3$, is defined by

$$\tilde{\mathbf{u}}(\mathbf{y}) = [N(\mathbf{y})]\,\tilde{\mathbf{u}} \quad , \tag{32}$$

in which the (3×24) real matrix $[N(\mathbf{y})]$ defines the interpolation functions and where the $\mathbb{R}^{24}$-vector $\tilde{\mathbf{u}}$ is made up of the degrees of freedom of the finite element. Let $\mathcal{I}$ be the set of indices defined by $\mathcal{I}=\{(i,j)\in\{(11),(22),(33),(12),(13),(23)\}\}$ and corresponding with the set $\mathfrak{I}=\{1,2,3,4,5,6\}$. From Eq. (32), it can be deduced that

$$\varepsilon_{ij}(\tilde{\mathbf{u}})\,(1-\delta_{ij})+\varepsilon_{ji}(\tilde{\mathbf{u}}) = [B(\mathbf{y})]_{Ik}\,\tilde{u}_k \quad ,(i,j)\in\mathcal{I}, I\in\mathfrak{I} \quad , \tag{33}$$

in which $[B(\mathbf{y})]$ is the (6×24) real matrix whose components are obtained by the calculation of partial derivatives of the interpolation functions contained in matrix $[N(\mathbf{y})]$.

The first step consists in calculating for each finite element the elementary contributions of the linear, quadratic and cubic internal forces projected on the POD-basis. Then, for a given finite element, the $\mathbb{R}^{24}$-vector constituted of the internal forces induced by the POD-basis vector $\boldsymbol{\varphi}^\beta$ and related to the linear stiffness term is written as

$$\tilde{\mathbf{f}}^{(1)}(\tilde{\boldsymbol{\varphi}}^\beta) = \sum_{i=1}^{r}[B(\mathbf{y}_i)]^T\,[D]\,[B(\mathbf{y}_i)]\,\tilde{\boldsymbol{\varphi}}^\beta\,(\det J)\,w_i \quad , \tag{34}$$

in which $\tilde{\boldsymbol{\varphi}}^\beta$ is the spatial restriction of POD-basis vector $\boldsymbol{\varphi}^\beta$ to the considered finite element, where $\mathbf{y}_i$, $i=\{1,\ldots,r\}$ are the locations of the r Gauss integration points related to the isoparametric finite element with w_i the corresponding weights and where $(\det J)$ is the Jacobian of the transformation from the considered finite element to the isoparametric one. Let $[C_k(\mathbf{y})]$ be the (3×24) real matrix defined by

$$\tilde{u}_{s,l}(\mathbf{y})\,\tilde{u}_{s,m}(\mathbf{y}) = \tilde{\mathbf{u}}^T\,[C_l(\mathbf{y})]^T\,[C_m(\mathbf{y})]\,\tilde{\mathbf{u}} \quad . \tag{35}$$

We then introduce the real (6×24) matrix $[E_\beta(\mathbf{y})]$ whose row number $I\in\mathfrak{I}$ is defined by

$$\tilde{\boldsymbol{\varphi}}^{\beta,T}\left([C_i(\mathbf{y})]^T\,[C_j(\mathbf{y})]\,(1-\delta_{ij})+[C_j(\mathbf{y})]^T\,[C_i(\mathbf{y})]\right) \quad . \tag{36}$$

Then, for a given finite element, the $\mathbb{R}^{24}$-vector constituted of the internal forces induced by the POD-basis vectors $\boldsymbol{\varphi}^\beta$ and $\boldsymbol{\varphi}^\gamma$ related to the quadratic stiffness term is written as

$$\tilde{\mathbf{f}}^{(2)}(\tilde{\boldsymbol{\varphi}}^\beta,\tilde{\boldsymbol{\varphi}}^\gamma) = \sum_{i=1}^{r}[B(\mathbf{y}_i)]^T\,[D]\,[E_\beta(\mathbf{y}_i)]\,\tilde{\boldsymbol{\varphi}}^\gamma\,(\det J)\,w_i) \quad . \tag{37}$$

In the same way, for a given finite element, the $\mathbb{R}^{24}$-vector constituted of the internal forces induced by the POD-basis vectors $\boldsymbol{\varphi}^\beta$, $\boldsymbol{\varphi}^\gamma$ and $\boldsymbol{\varphi}^\delta$ and related to the cubic stiffness term is written as

$$\tilde{\mathbf{f}}^{(3)}(\tilde{\boldsymbol{\varphi}}^\beta,\tilde{\boldsymbol{\varphi}}^\gamma,\tilde{\boldsymbol{\varphi}}^\delta) = \sum_{i=1}^{r}[E_\beta(\mathbf{y}_i)]^T\,[D]\,[E_\gamma(\mathbf{y}_i)]\,\tilde{\boldsymbol{\varphi}}^\delta\,(\det J)\,w_i \quad . \tag{38}$$

In a second step, for each type of stiffness, we proceed with the assembly of each of these elementary contributions. We then denote by $\mathbf{f}^{(1)}(\boldsymbol{\varphi}^\beta)$, $\mathbf{f}^{(2)}(\boldsymbol{\varphi}^\beta,\boldsymbol{\varphi}^\gamma)$ and $\mathbf{f}^{(3)}(\boldsymbol{\varphi}^\beta,\boldsymbol{\varphi}^\gamma,\boldsymbol{\varphi}^\delta)$ the $\mathbb{R}^n$-vectors of these internal loads. The mean reduced nonlinear computational model is then described by

$$\mathcal{K}^{(1)}_{\alpha\beta} = \boldsymbol{\varphi}^{\alpha,T}\,\mathbf{f}^{(1)}(\boldsymbol{\varphi}^\beta) \quad , \tag{39}$$

$$\hat{\mathcal{K}}^{(2)}_{\alpha\beta\gamma} = \boldsymbol{\varphi}^{\alpha,T}\,\mathbf{f}^{(2)}(\boldsymbol{\varphi}^\beta,\boldsymbol{\varphi}^\gamma) \quad , \tag{40}$$

$$\mathcal{K}^{(3)}_{\alpha\beta\gamma\delta} = \boldsymbol{\varphi}^{\alpha,T}\,\mathbf{f}^{(3)}(\boldsymbol{\varphi}^\beta,\boldsymbol{\varphi}^\gamma,\boldsymbol{\varphi}^\delta) \quad . \tag{41}$$

The quadratic stiffness contribution $\mathcal{K}^{(2)}_{\alpha\beta\gamma}$ of the mean reduced nonlinear computational model is then build from Eq. (16). It should be noted that the $\mathcal{K}^{(1)}_{\alpha\beta}$, $\hat{\mathcal{K}}^{(2)}_{\alpha\beta\gamma}$ and $\mathcal{K}^{(3)}_{\alpha\beta\gamma\delta}$ contributions have to be explicitly known for constructing the uncertain nonlinear computational model in the general case of complex structures.

4 NONPARAMETRIC STOCHASTIC MODELING OF UNCERTAINTIES

In this Section, it is assumed that the mean reduced nonlinear computational model contains both system parameter uncertainties and model uncertainties which justifies the use of the nonparametric probabilistic approach for modeling these uncertainties in the computational model. The main idea of the nonparametric probabilistic approach consists in replacing each of the matrices of a given mean reduced computational model by a random matrix whose probability model is constructed from the maximum entropy principle using the available information [12], [13]. In the usual linear case, the random matrices issued from the mechanical system are with values in the set of the symmetric positive-definite matrices. In the present geometrical nonlinear context, the nonlinear equations involve nonlinear operators. In this case, we then introduce the matrix $[\mathcal{K}]$ [9] as the real $(P\times P)$ matrix with $P=N(N+1)$ defined by

$$[\mathcal{K}] = \begin{bmatrix} [\mathcal{K}^{(1)}] & [\hat{\mathcal{K}}^{(2)}] \\ [\hat{\mathcal{K}}^{(2)}]^T & 2\,[\mathcal{K}^{(3)}] \end{bmatrix} \quad , \tag{42}$$

in which $[\hat{\mathcal{K}}^{(2)}]$ and $[\mathcal{K}^{(3)}]$ are respectively the $(N\times N^2)$ and $(N^2\times N^2)$ real matrices resulting from the following reshaping operation defined by

$$[\hat{\mathcal{K}}^{(2)}]_{\alpha J} = \hat{\mathcal{K}}^{(2)}_{\alpha\beta\gamma} \quad , \quad \text{with } J=(\beta-1)N+\gamma \quad , \tag{43}$$

$$[\mathcal{K}^{(3)}]_{IJ} = \mathcal{K}^{(3)}_{\alpha\beta\gamma\delta} \text{ with } I=(\alpha-1)N+\beta \text{ and } J=(\gamma-1)N+\delta. \tag{44}$$

It is shown in [9] that matrix $[\mathcal{K}]$ is a symmetric positive-definite matrix. Consequently, the nonparametric probabilistic approach can easily be adapted to the geometrically nonlinear context as follows. The mean reduced matrix $[\mathcal{K}]$ is replaced by the random matrix $[\boldsymbol{\mathcal{K}}]$ such that $\mathcal{E}\{[\boldsymbol{\mathcal{K}}]\}=[\mathcal{K}]$ in which $\mathcal{E}$ is the mathematical expectation. The random matrix $[\boldsymbol{\mathcal{K}}]$ is then written as $[\boldsymbol{\mathcal{K}}]=[L_K]^T\,[\mathbf{G}_K]\,[L_K]$ in which $[L_K]$ is a $(P\times P)$ real upper matrix such that $[\mathcal{K}]=[L_K]^T\,[L_K]$ and where $[\mathbf{G}_K]$ is a full random matrix with value in the set of all the positive-definite symmetric $(P\times P)$ matrices. The probability model of random matrix $[\mathbf{G}_K]$ is constructed by using the maximum entropy principle with the available information. All details concerning the construction of this probability model can be found in [12], [13]. The dispersion of random matrix $[\mathbf{G}_K]$ is controlled by one real positive parameter $\delta \in \mathcal{D}$ called the dispersion parameter. In addition, there exists an algebraic representation of this random matrix useful to the Monte Carlo numerical simulation. From random matrix $[\mathcal{K}]$ the random linear, quadratic and stiffness terms $\mathcal{K}^{(1)}_{\alpha\beta}$, $\hat{\mathcal{K}}^{(2)}_{\alpha\beta\gamma}$ and $\mathcal{K}^{(3)}_{\alpha\beta\gamma\delta}$ can easily be deduced. The random matrix model is then defined by

$$\mathbf{U} = [\Phi^N]\,\mathbf{Q} \quad , \tag{45}$$

in which $\mathbf{Q} = (\mathbf{Q}_1, \ldots, \mathbf{Q}_N)$ is the $\mathbb{R}^N$-valued vector of the random generalized coordinates solution of the random equation

$$\mathcal{K}^{(1)}_{\alpha\beta}\,\mathbf{Q}_\beta + \mathcal{K}^{(2)}_{\alpha\beta\gamma}\mathbf{Q}_\beta\,\mathbf{Q}_\gamma + \mathcal{K}^{(3)}_{\alpha\beta\gamma\delta}\mathbf{Q}_\beta\,\mathbf{Q}_\gamma\,\mathbf{Q}_\delta = \mathcal{F}_\alpha \quad , \tag{46}$$

with

$$\mathcal{K}^{(2)}_{\alpha\beta\gamma} = \frac{1}{2}\big(\hat{\mathcal{K}}^{(2)}_{\alpha\beta\gamma} + \hat{\mathcal{K}}^{(2)}_{\beta\gamma\alpha} + \hat{\mathcal{K}}^{(2)}_{\gamma\alpha\beta}\big) \quad . \tag{47}$$

5 IDENTIFICATION OF THE UNCERTAIN NONLINEAR COMPUTATIONAL MODEL

In this Section, the identification of the uncertain nonlinear computational model from experimental data is formulated. It is assumed that the mean reduced nonlinear computational is known and that the identification focuses on the parameter δ controlling the uncertainty level in the uncertain computational model. This robust updating problem consists then in minimizing a cost function with respect to parameter δ. The formulation of the optimization problem requires the definition of a cost function relevant to the uncertain nonlinear computational model and to the experimental data. In the present case, it is proposed here to introduce penalty terms only in areas for which the experimental data is not within the confidence region constructed with the uncertain nonlinear computational model. It is assumed that a collection of n_{exp} experimental responses are available at n_{obs} spatial locations. We then denote as $U^{exp}_j(s,\theta_k)$ the experimental response number k at dof number j as a function of the load increment s. The corresponding observation issued from the uncertain computational model is denoted as $U_j(\delta,s)$ and is a function of the parameter δ to be updated. Let $U^+_j(\delta,s)$ (resp. $U^-_j(\delta,s)$) and $U^{exp,+}_j(s)$ (resp. $U^{exp,-}_j(s)$) be the upper (resp. lower) envelope of the confidence region of observation $U_j(\delta,s)$ obtained with a probability level $\alpha = 0.95$ and the upper (resp. lower) envelope of experiments $U^{exp}_j(s)$. The cost function $j(\delta)$ is then defined by

$$j(\delta) = ||\mathbf{\Delta}^+(\delta,\cdot)||^2_{\mathbb{B}} + ||\mathbf{\Delta}^-(\delta,\cdot)||^2_{\mathbb{B}} \quad , \tag{48}$$

in which $||\cdot||_{\mathbb{B}}$ is the $\mathcal{L}^2$ norm over the load incremental band $\mathbb{B} = [0,b]$ and where $\mathbf{\Delta}^+(\delta,s)$ and $\mathbf{\Delta}^-(\delta,s)$ are the $\mathbb{R}^{n_{obs}}$-vectors whose component number j is defined by

$$\begin{aligned}\Delta^+_j(\delta,s) = \quad & \{U^+_j(\delta,s) - U^{exp,+}_j(s)\} \times \\ & \{1 - H(U^+_j(\delta,s) - U^{exp,+}_j(s))\} \quad ,\end{aligned} \tag{49}$$

$$\begin{aligned}\Delta^-_j(\delta,s) = \quad & \{U^-_j(\delta,s) - U^{exp,-}_j(s)\} \times \\ & \{H(U^-_j(\delta,s) - U^{exp,+}_j(s)))\} \quad ,\end{aligned} \tag{50}$$

where $x \mapsto H(x)$ is the Heaviside function. The identification of the uncertain nonlinear computational model consists then in solving the optimization problem

$$\text{find } \delta^{opt} \in \mathcal{D} \text{ such that } j(\delta^{opt}) \leq j(\delta) \quad , \quad \forall \delta \in \mathcal{D}.$$

6 NUMERICAL APPLICATION

The objective of this application is to show the capability of the presented methodology in the context of the robust identification of an uncertain nonlinear computational model with respect to given experimental data. The numerical example consists in a three-dimensional linear elastostatic problem in the geometrically nonlinear context. For clarity, the material is chosen to be homogeneous and isotropic, the extension to the nonhomogeneous case and to the anisotropic case is straightforward. A preliminary calculation is carried out with MD NASTRAN in order to get the reference solution from which the POD-basis is deduced. The uncertain nonlinear computational model is then constructed as a function of identification parameter δ as described in the theoretical part of the paper. The experimental data basis has been obtained by numerical simulations with MD NASTRAN. Note that the geometrical characteristics of the structure have been modified and that the material characteristics have been chosen to be inhomogeneous so that it is impossible for the uncertain nonlinear computational model to be identified to match the experimental data.

6.1 Mean finite element model

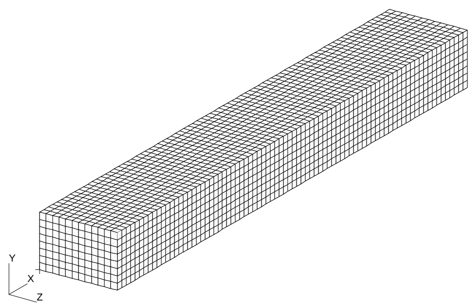

Figure 1. Finite element model

The three-dimensional bounded domain Ω is a slender domain such that $\Omega =]0,L[\times]0,b[\times]0,h[$ in a cartesian system defined by $(0,\mathbf{e}_1,\mathbf{e}_2,\mathbf{e}_3)$ with $L = 10\,m$, $b = 1\,m$ and $h = 1.5\,m$. Let $\Gamma_0 \subset \partial\Omega$ be the boundary described as $\{x_1 = 0, x_2 \in [0,b]\,, x_3 \in [0,h]\,\}$. Since the structure is fixed on section $x_1 = 0$, we have a Dirichlet condition on boundary Γ_0. The structure is free on section $x_1 = 10\,m$. The structure is subjected to external surface loads applied along both directions $\mathbf{e}_1$ and $\mathbf{e}_2$ in the end section defined by $x_1 = 10\,m$. The Young modulus and the Poisson coefficient related to the homogeneous and isotropic linear elastic material are $E = 10^{10}\,N.m^{-2}$ and $\nu = 0.15$. The finite element model is a regular mesh of 9477 nodes and

$80 \times 8 \times 12 = 7680$ finite elements constituted of 8-nodes solid elements with $r = 8$ Gauss integration points. Therefore, the mean computational model has $n = 28080$ degrees of freedom (see figure 1). The discretization of the external loads yields point loads applied on the nodes of the end section along the direction $\mathbf{e}_2$ with intensity $f = 4\,000\,000\,N$ and yields point loads applied on the nodes of the end section along the direction $\mathbf{e}_1$ with intensity $f = -500\,000\,N$. An initial imperfection with a maximum amplitude of $200\,\mu m$ is added to the initial structure in order to construct the mean nonlinear computational model. This initial imperfection is defined by the first buckling mode of the initial structure. In the present case, the first buckling mode is a bending mode with eigenvalue $\lambda_c = 0.371$ corresponding to a critical load $f_c = 1\,484\,000\,N$ along the direction $\mathbf{e}_2$ (respectively $f_c = -185\,000\,N$ along the direction $\mathbf{e}_1$). Then, the mean nonlinear computational model corresponds to a slightly curved beam whose shape is zoomed and shown in the figure 2.

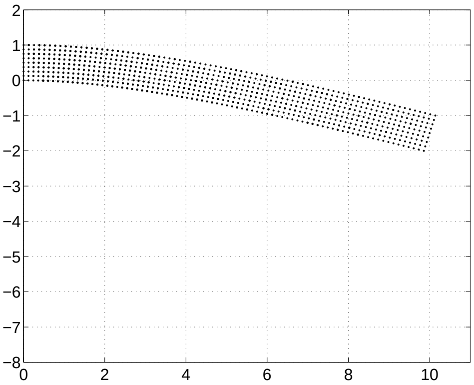

Figure 2. Finite element model of the curved beam.

In order to simulate the post-buckling mechanical behavior, the static nonlinear calculations are carried out by solving Eq. (25) using MD NASTRAN with algorithms based on the arc-length method. The displacement field is calculated using $n_t = 110$ load increments. Figure 3 shows the static displacement field of the structure in the geometrically nonlinear case.

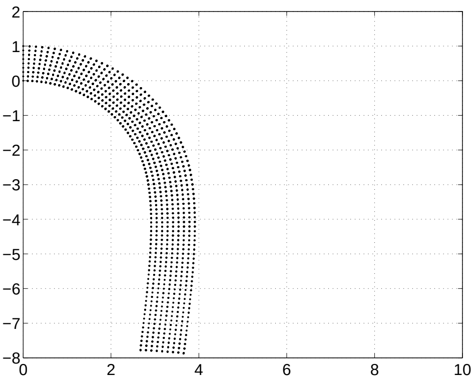

Figure 3. static displacement field of the structure

6.2 Construction of the experimental data basis

It is assumed that $n_{exp} = 6$ experimental measurements of the static nonlinear response are available. The measurements are performed at $n_{obs} = 1$ observation point at the middle of the end section in the direction $(0, \mathbf{e}_2)$. The experimental static response is denoted by $u_{obs}^{exp,k}(s)$, $k \in 1, \ldots, n_{exp}$. The corresponding quantity defined for the mean nonlinear computational model is denoted as $u_{obs}(s)$. The experimental data is generated as follows. Assuming the existence of geometrical tolerances of 5% around the geometrical characteristics, the maximum entropy principle transform the geometrical parameters L, b and h by the random variables L, B and H with uniform probability density function centered around the mean characteristics and with standard deviation taken as $\sigma_L = \dfrac{0.05\,L}{\sqrt{3}}$, $\sigma_b = \dfrac{0.05\,b}{\sqrt{3}}$ and $\sigma_h = \dfrac{0.05\,h}{\sqrt{3}}$ respectively. Moreover, assuming the Young modulus to be inhomogeneous with 10% of variation around its mean value is achieved by replacing its deterministic value by a stochastic field $E(\mathbf{x})$. The stochastic field is simply modeled by

$$E(\mathbf{x}) = E + \sum_{j=1}^{J} \xi_j \mathbf{b}_j(\mathbf{x}) \quad , \tag{51}$$

in which ξ_j, $j \in \{1, \ldots, J\}$ are independent uniform random variables with zero mean and standard deviation $\sigma = \dfrac{0.1\,E}{\sqrt{3}}$ and where the functions $\mathbf{b}_j(\mathbf{x})$ are given basis functions. For convenience, these smooth functions are taken as the spatial average over each element of the eigenvectors related to the J lowest eigenvalues of the usual linear generalized eigenvalue problem.

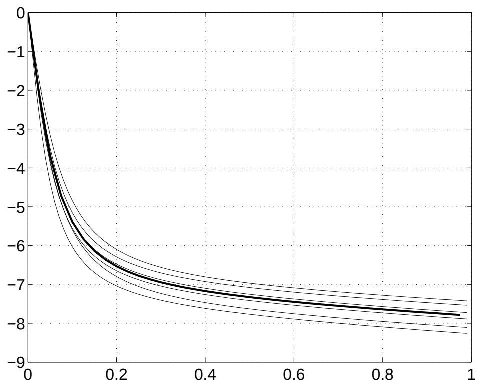

Figure 4. response of the observation point as a function of the incremental load: mean computational model (thick line), experimental data (thin lines)

Figure 4 compares the static nonlinear response as a function of the incremental load for both mean nonlinear computational model and experimental measurements. Since the experimental nonlinear responses are widespread around the response of the mean nonlinear computational model, it can be seen that the use of an uncertain nonlinear computational model is perfectly justified.

6.3 Construction of the reduced order basis

The nonlinear response shown in Figure 3 is then used for calculating the POD-basis as described in Section 3. Let $Conv - POD(N)$ be the function defined by

$$Conv - POD(N) = 1 - \frac{tr([\Lambda^N])}{tr([A])} \quad , \qquad (52)$$

for which the calculation of $tr([A])$ is obtained without computing matrix $[A]$. Figure 5 shows the graph $N \mapsto Conv - POD(N)$. It can be seen that the convergence is quickly obtained. Henceforth, all the numerical calculations are carried out with $N = 4$ POD-basis vectors. The mean reduced nonlinear computational model is then constructed and the static nonlinear equations are solved using the numerical algorithm of Crisfield [19] based on the arc-length method. It can be seen that the prediction error between the mean nonlinear computational model and between its reduced counterpart at the observation point is less than 0.06%.

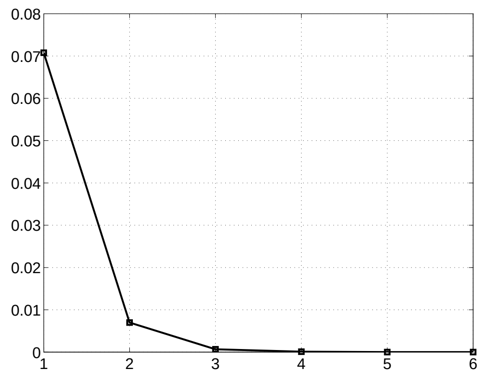

Figure 5. Convergence analysis : graph of $N \mapsto Conv - POD(N)$.

6.4 Experimental identification of the uncertain nonlinear computational model

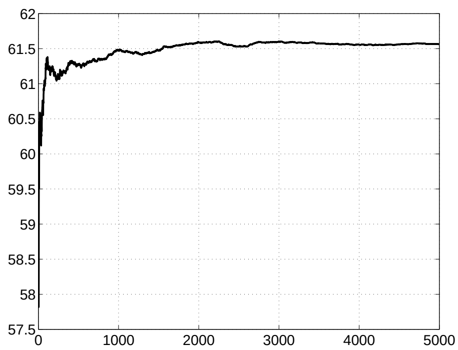

Figure 6. Convergence analysis : graph of $n_s \mapsto Conv(n_s)$.

The construction of the uncertain nonlinear computational model using the nonparametric probabilistic approach is performed as explained in Section 4. A stochastic convergence analysis is then carried out to define the number n_s of Monte Carlo realizations to be kept in the numerical simulation. Let $n_s \mapsto Conv(n_s)$ be the function defined by

$$Conv(n_s) = \frac{1}{n_s}\Big\{ \sum_{j=1}^{n_s} |||\mathbf{U}(\theta_j)|||^2 \Big\}^{1/2} \quad , \qquad (53)$$

in which $|||\mathbf{U}(\theta_j)||| = \max_s ||\mathbf{U}(\theta_j, s))||$, $||\mathbf{U}(\theta_j, s))||^2 = \sum_{k=1}^{n} U_k^2(\theta_j, s)$ with $U_k(\theta_j, s)$ the realization number j of the random response at dof number k for a given load increment s. Figure 6 displays the graph $n_s \mapsto Conv(n_s)$ obtained with a dispersion parameter $\delta = 0.6$. Convergence is reached for $n_s = 3000$. The robust identification is then carried out by studying the non-differentiable cost function $\delta \mapsto j(\delta)$ with direct Monte Carlo numerical simulations. Since only one observation point is available, this means that the cost function is a positive decreasing function of the parameter δ. As soon as the experimental data basis belongs to the confidence region of the random observation, the cost function is equal to zero.

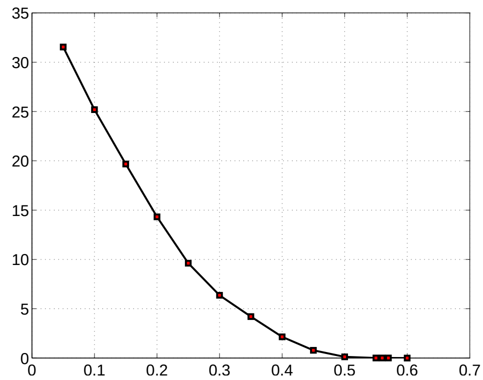

Figure 7. Robust identification : graph of $\delta \mapsto j(\delta)$.

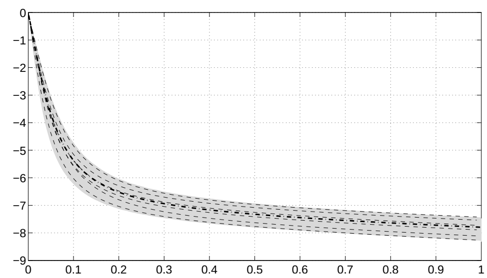

Figure 8. Robust identification : graph of the experimental data $s \mapsto u_{obs}^{exp,k}(s)$ (thin dashed lines), graph of the mean response $s \mapsto u_{obs}(s)$ (thick dashed line), graph of the confidence region of the random response $s \mapsto U_{obs}(s)$ (grey region).

Figure 7 shows the cost function $\delta \mapsto j(\delta)$. It can be seen that the optimal value is given by $\delta^{opt} = 0.56$. Figure 8 displays the graph of the confidence region of the optimal random response $U_{obs}(\delta^{opt}, s)$ as a function of the load increment s. It can be seen that there is a good agreement between the optimal uncertain nonlinear computational model and between the experimental data basis.

7 CONCLUSION

In the present paper, a methodology has been proposed for constructing an uncertain nonlinear computational model for any three-dimensional structure in the context of linear elastostatics with geometric nonlinearity. The mean reduced nonlinear computational model is constructed by projection on the POD-basis obtained from a reference calculation. All the integrals involved in the weak formulation after projection on the POD-basis are explicitly estimated using three-dimensional solid finite elements. The construction of each contribution in the quadratic term allows the uncertain nonlinear computational model based on the nonparametric probabilistic theory to be constructed in any case. A numerical example carried out in the context of the robust identification of an uncertain computational model with respect to an experimental basis shows the efficiency of the method.

REFERENCES

[1] P. Pai, A. Nayfeh, A Fully Nonlinear-Theory of Curved And Twisted Composite Rotor Blades Accounting For Warpings and 3-Dimensional Stress Effects, International Journal of Solids and Structures 31 (9) (1994) 1309–1340.

[2] D. Tang, E. Dowell, Nonlinear response of a non-rotating rotor blade to a periodic gust, Journal of Fluids and Structures 10 (7) (1996) 721–742.

[3] D. Hodges, X. Shang, C. Cesnik, Finite element solution of nonlinear intrinsic equations for curved composite beams, Journal of the American Helicopter Society 41 (4) (1996) 313–321.

[4] E. Lindgaard, E. Lund, K. Rasmussen, Nonlinear buckling optimization of composite structures considering “worst” shape imperfections, International Journal of Solids and Structures 47 (22-23) (2010) 3186–3202.

[5] H. Huang, Q. Han, Research on nonlinear postbuckling of functionally graded cylindrical shells under radial loads, Computers & Structures 92 (6) (2010) 1352–1357.

[6] R. Sampaio, C. Soize, Remarks on the efficiency of pod for model reduction in non-linear dynamics of continuous elastic systems, International Journal for Numerical Methods in Engineering 72 (1) (2007) 22–45.

[7] J. J. Hollkamp, R. W. Gordon, Reduced-order models for nonlinear response prediction: Implicit condensation and expansion, Journal of Sound and Vibration 318 (4-5) (2008) 1139–1153.

[8] A. Muryavov, S. Rizzi, Determination of nonlinear stiffness with application to random vibration of geometrically nonlinear structures, Computers & Structures 81 (2003) 1513–1523.

[9] M.-P. Mignolet, C. Soize, Stochastic reduced order models for uncertain geometrically nonlinear dynamical systems, Computer Methods in Applied Mechanics and Engineering 197 (2008) 3951–3963.

[10] C. Schenk, G. Schuëller, Buckling analysis of cylindrical shells with random geometric imperfections, International Journal of Nonlinear Mechanics 38 (7) (2003) 1119–1132.

[11] C. Schenk, G. Schuëller, Buckling analysis of cylindrical shells with cutouts including random boundary and geometric imperfections, Computer Methods in Applied Mechanics and Engineering 196 (35-36) (2007) 3424–3434.

[12] C. Soize, A nonparametric model of random uncertainties for reduced matrix models in structural dynamics, Probabilistic Engineering Mechanics 15 (3) (2000) 277–294.

[13] C. Soize, A comprehensive overview of a non-parametric probabilistic approach of model uncertainties for predictive models in structural dynamics, Journal of Sound and Vibration 288 (3) (2005) 623–652.

[14] R. Murthy, X. Wang, M.-P. Mignolet, Uncertainty-based experimental validation of nonlinear reduced order models, in: Proceedings of the RASD 2010, Southampton, 12-14 July 2010, 2010.

[15] C. Soize, E. Capiez-Lernout, J.-F. Durand, C. Fernandez, L. Gagliardini, Probabilistic model identification of uncertainties in computational models for dynamical systems and experimental validation., Computer Mechanical Methods in Applied Mechanics and Engineering 98 (1) (2008) 150–163.

[16] E. Capiez-Lernout, C. Soize, Robust updating of uncertain damping models in structural dynamics for low- and medium-frequency ranges., Mechanical Systems and Signal Processing 22 (8) (2008) 1774–1792.

[17] L. Sirovich, turbulence and the dynamics of coherent structures .1. coherent structures, quarterly of applied mathematics 45 (3) (1987) 561–571.

[18] S.-H. Lee, MSC/Nastran Handbook for nonlinear analysis, version 67, Lee, S.-H. editor, 1992.

[19] M. Crisfield, Non-linear finite element analysis of solids and structures, Vol. 1 : essentials, John Wiley and Sons, Chichester, 1997.

[20] J. Yvonnet, H. Zahrouni, M. Potier-Ferry, A model reduction method for the post-buckling analysis of cellular microstructures, Computer Methods in Applied Mechanics and Engineering 197 (2007) 265–280.